Dynamical response of a dipole near the surface of a nonlocal metal

R. Fuchs

Ames Laboratory, United States Department of Energy, Iowa State University, Ames, Iowa 50011
and Department of Physics, Iowa State University, Ames, Iowa 50011

R. G. Barrera

Institute of Physics, University of Mexico, Mexico 20, D. F., Mexico

(Received 2 April 1981)

Expressions are derived for the potential of an oscillating point charge near the surface of a metal described by a nonlocal dielectric constant. The induced field at the site of a dipole outside the surface is found, and this result is used to calculate the renormalized polarizability of a dipole oscillator. Calculations are carried out using a hydrodynamic nonlocal dielectric constant, and the effects of nonlocal surface-plasmon dispersion and coupling to bulk plasmons are apparent. Expressions for the potential are also found if the added charge is placed within the nonlocal medium.

I. INTRODUCTION

A knowledge of the optical behavior of atoms and molecules near the surface of a metal is important for understanding effects such as surface-enhanced Raman scattering[1-3] and differential reflectance spectroscopy of adsorbed atoms.[4,5] Several theories have been developed for the effect of a metal surface on the radiation of a dipole oscillator[6,7] and on the reflectance spectrum of an adsorbed overlayer of atoms[8] in which the metal is described by a local dielectric constant $\epsilon(\omega)$. This local description will become invalid if the dipoles are within a few Å of the surface. There has been much work recently on the static ($\omega = 0$) nonlocal response of a metal to a charge near the surface using the random-phase approximation (RPA) with a jellium model of the metal,[9-11] but these theories cannot be extended readily to nonzero frequencies.

We shall address the following problem. An atom, considered as a point dipole oscillating with frequency ω, is situated outside a metal surface. The dipole induces oscillating image charges in the metal which in turn produce an induced electric field at the site of the dipole. We wish to determine this induced field as a function of the frequency, the properties of the metal, and the distance of the dipole from the surface. This field changes the unrenormalized frequency-dependent polarizability $\alpha_0(\omega)$ of the atomic dipole at an infinite distance from the metal to a renormalized polarizability $\alpha(\omega)$ that is related to the optical-absorption spectrum of

the atom near the surface.[8] We shall neglect retardation, so our results will be valid only if the distance of the dipole to the surface is much smaller than the wavelength of light.

A general formalism for solving this problem has been set up by Feibelman.[12] He uses an RPA jellium description of the metal, which he takes to be Al, but is able to calculate the induced field only if the dipole is far from the metal surface. This is a severe limitation arising from a long-wavelength expansion which requires that the electric field have appreciable Fourier components only for small values of the wave vector q_1 parallel to the surface. We believe that this limitation excludes some of the more interesting effects of nonlocality, namely the dispersion of the surface and bulk-plasmon modes and the appearance of electron-hole pair excitations at the large values of q_1 that occur when the dipole is close to the surface. It is also difficult to generalize Feibelman's theory to other metals and to include electron scattering in the metal.

A general theory for the screening for an oscillatory dipole near a metal surface has also been developed by Korzeniewski, Maniv, and Metiu.[13] Using an infinite-barrier model to calculate the nonlocal dielectric response of the metal, they have found the induced electric field at a number of frequencies for various locations of the dipole and the field point.

We have chosen to describe the metal with the specular scattering or semiclassical infinite-barrier (SCIB) model.[14,15] Although this model does not

treat the diffuse nature of the metal surface correctly, it includes the most important effects of nonlocality, it can be solved easily for arbitrary distance of the dipole from the surface and for different metals, and the results can be understood physically. There are two interesting effects that appear when the dipole approaches the surface: (1) The singularity in the image dipole in a local theory (and also in Feibelman's results) that occurs when the dielectric constant of the metal is $\epsilon(\omega) = -1$, is removed because of surface-plasmon dispersion at large values of q_1. (2) An additional damping mechanism appears at frequencies higher than the plasma frequency because of generation of bulk plasmons. The SCIB model of the metal cannot be expected to be valid if the dipole approaches to within $1-2$ Å of the surface; however, for such small distances the point dipole picture of an atom also will be incorrect and there will be complicating effects due to overlap of the atomic wave functions with the metal.[12]

In Sec. II we place a point charge outside the metal and derive expressions for the potential at all points in space in terms of the longitudinal dielectric constant $\epsilon_l(\vec{q},\omega)$ of the metal. We use this result to find the electric field produced by the image charges for a dipole outside the metal. This induced field at the location of the dipole will renormalize the polarizability of the dipole.

Our expressions for the induced field are special cases of those found originally by Sommerfeld[16,17] in his treatment of a dipole above a conducting plane, although Sommerfeld did not explicitly use a nonlocal dielectric constant. If the reflectance amplitude is known for *all* values of the wave vector q_1 parallel to the surface, the induced field outside the surface can be determined with retardation included. That is, the nonlocality of the metal enters only into the expression for the reflectance amplitude, and not into the relationship between the reflectance amplitude and the induced field. This fact is implicit in the work of Chance et al.[18] and Tews,[19] and it has been explicitly noted by Weber and Ford[20] who have emphasized the essential role of nonlocality in the image dipole model of surface-enhanced Raman scattering. Although the work of Weber and Ford[20] has some similarity to ours, they proceed directly to the Raman scattering problem and do not present calculations of the induced field, nor do they include any frequency dependence of the unrenormalized polarizability α_0. An equivalent method has been used by Agarwal and Wolmer[21] to calculate the radiative lifetime of an atom near the surface of

a metal described by a hydrodynamic nonlocal dielectric constant.

Section III presents numerical calculations using a hydrodynamic model for the dielectric constant of the metal and a simple harmonic-oscillator dipole polarizability. In the Appendix we find expressions for the potential produced by a point charge *inside* the metal. These results can be used to treat the influence of the surface on screened interactions between impurities or vacancies as well as the interaction of such defects with the surface itself.

II. GENERAL THEORY USING THE SCIB MODEL

A. Potential produced by an oscillating point charge

We set up a coordinate system such that the metal, described by a nonlocal dielectric constant, fills the half-space $z > 0$ and a medium with a local dielectric constant $\epsilon_0(\omega)$, which we will usually consider to be vacuum, fills the half-space $z < 0$. An oscillating point charge $Q(t) = Q_0 \exp(-i\omega t)$ is located at the point $(0,0,-z_0)$ outside the metal. The distance z_0 between the charge and the metal surface is restricted to be much smaller than the wavelength of light, so retardation can be neglected; i.e., $\vec{B} = 0$, $\vec{\nabla} \times \vec{E} = 0$, and $\vec{E}$ can be derived from a scalar potential ϕ. The charge and all fields have a common time dependence $\exp(-i\omega t)$ which will not be written explicitly.

Outside the metal, the potential $\phi(\vec{r})$ can be written

$$\phi(\vec{r}) = \phi_0(\vec{r}) + \phi'(\vec{r}) , \tag{1}$$

where

$$\phi_0(\vec{r}) = \frac{Q}{\epsilon_0 |\vec{r} + z_0\hat{k}|} \tag{2}$$

is the potential produced by the point charge and $\phi'(\vec{r})$ is the potential produced by the charge induced in the metal. It will be convenient to Fourier transform all potentials and fields from the two-dimensional spatial vector $\vec{\rho} = x\hat{i} + y\hat{j}$ to the corresponding wave vector $\vec{q}_1 = q_x\hat{i} + q_y\hat{j}$. For the potential ϕ_0 we find

$$\phi_0(\vec{q}_1,z) = \int e^{-i\vec{q}_1 \cdot \vec{\rho}} \phi_0(\vec{r})dx\,dy \tag{3a}$$

$$= \frac{2\pi Q}{\epsilon_0 q_1} e^{-q_1|z+z_0|} . \tag{3b}$$

The source of the potential $\phi'(\vec{r})$ is the charge induced in the metal, so $\phi'(\vec{r})$ is a solution of Laplace's equation $\nabla^2\phi' = 0$ for $z < 0$. The Fourier

component $\phi'(q_1,z)$ must therefore satisfy the equation

$$\left[\frac{d^2}{dz^2} - q_1^2\right]\phi'(\vec{q}_1,z) = 0 .$$ (4)

The solution is of the form

$$\phi'(\vec{q}_1,z) = C_1 e^{q_1 z} + C_2 e^{-q_1 z} ,$$ (5)

where the term $C_2 e^{-q_1 z}$ must be discarded because $\phi' \to 0$ as $z \to -\infty$. Adding Eqs. (3b) and (5), we find the total potential outside the metal,

$$\phi(\vec{q}_1,z) = \frac{2\pi Q}{\epsilon_0 q_1} e^{-q_1|z+z_0|} + C_1 e^{q_1 z}, \quad z < 0$$ (6)

where the unknown quantity C_1 will be determined from boundary conditions at $z = 0$.

We now consider the potential inside the metal. Using the SCIB model we temporarily imagine the metal to be extended throughout all space and impose the symmetry conditions $E_x(\vec{\rho},z) = E_x(\vec{\rho},-z)$, $E_y(\vec{\rho},z) = E_y(\vec{\rho},-z)$, and $E_z(\vec{\rho},z) = -E_z(\vec{\rho},-z)$, with similar conditions for the displacement $\vec{D}(\vec{\rho},z)$. There is no added charge in the metal, so $\vec{\nabla}\cdot\vec{D} = 0$ for both $z > 0$ and $z < 0$. However, because of the symmetry conditions, D_z is discontinuous at $z = 0$, so we must imagine an added fictitious charge layer[22] at $z = 0$ that acts as a source for a "potential" $\phi_D(\vec{r})$ from which $\vec{D}$ can be derived: $\vec{D} = -\vec{\nabla}\phi_D$. Poisson's equation for ϕ_D is

$$\nabla^2\phi_D(\vec{r}) = -4\pi f(\vec{\rho})\delta(z) ,$$ (7)

where $f(\vec{\rho})$ is the unknown fictitious surface charge density. The three-dimensional Fourier transform of Eq. (7) is

$$-q^2\phi_D(\vec{q}) = -4\pi f(\vec{q}_1) ,$$ (8)

where $q^2 = q_1^2 + q_z^2$ and

$$f(\vec{q}_1) = \int e^{-i\vec{q}_1\cdot\vec{\rho}} f(\vec{\rho})dx\, dy .$$ (9)

From Eq. (8) we immediately find

$$\phi_D(\vec{q}) = 4\pi f(\vec{q}_1)/q^2$$ (10)

and the displacement

$$\mathscr{D}_z(\vec{q}) = -iq_z\phi_D(\vec{q})$$

$$= -4\pi i f(\vec{q}_1)q_z/q^2 .$$ (11)

The $q_z \to \infty$ limit of $\mathscr{D}_z(\vec{q})$ gives the value of D_z just inside the surface of the metal,[23]

$$D_z(\vec{q}_1,z = 0^+) = \frac{i}{2}\lim_{q_z\to\infty} q_z\mathscr{D}_z(\vec{q})$$ (12)

$$= 2\pi f(\vec{q}_1) ,$$ (13)

so Eq. (10) can be written

$$\phi_D(\vec{q}) = 2D_z(\vec{q}_1,0^+)/q^2 .$$ (14)

The potential $\phi(\vec{r})$, from which the electric field can be derived $(\vec{E} = -\nabla\phi)$, has the Fourier transform $\phi(\vec{q})$ found by dividing $\phi_D(\vec{q})$ by the bulk longitudinal dielectric constant:

$$\phi(\vec{q}) = \frac{2D_z(\vec{q}_1,0^+)}{q^2\epsilon_l(\vec{q},\omega)} .$$ (15)

The transformed potential, defined by

$$\phi(\vec{q}_1,z) = \frac{1}{2\pi}\int_{-\infty}^{\infty} \phi(\vec{q})e^{iq_z z}dq_z ,$$ (16)

has the value

$$\phi(\vec{q}_1,0^+) = \frac{D_z(\vec{q}_1,0^+)}{\pi}\int_{-\infty}^{\infty} \frac{dq_z}{q^2\epsilon_l(\vec{q},\omega)}$$ (17)

just inside the surface of the metal.

Returning to the physical two-medium system, we now impose the boundary conditions that (1) the tangential component of the electric field (or equivalently, the potential) and (2) the normal component of the displacement be continuous at $z = 0$. The first boundary condition gives, from Eqs. (6) and (17),

$$\frac{2\pi Q}{\epsilon_0 q_1}e^{-q_1 z_0} + C_1 = \frac{D_z(\vec{q}_1,0^+)}{\pi}\int_{-\infty}^{\infty} \frac{dq_z}{q^2\epsilon_l(\vec{q},\omega)} .$$ (18)

The normal component of the displacement outside the surface is

$$D_z(\vec{q},z) = -\epsilon_0(\partial/\partial z)\phi(\vec{q}_1,z) ,$$

therefore from Eq. (6) the second boundary condition gives

$$2\pi Qe^{-q_1 z_0} - \epsilon_0 q_1 C_1 = D_z(\vec{q}_1,0^+) .$$ (19)

Combining Eqs. (18) and (19) we find

$$C_1 = \frac{2\pi Qe^{-q_1 z_0}}{\epsilon_0 q_1}B(q_1) ,$$ (20)

$$D_z(\vec{q}_1,0^+) = 2\pi Qe^{-q_1 z_0}\frac{2}{\epsilon_0 I(q_1) + 1} ,$$ (21)

where[24]

$$I(q_1) = \frac{q_1}{\pi}\int_{-\infty}^{\infty} \frac{dq_z}{q^2\epsilon_l(\vec{q},\omega)}$$ (22)

and

$$B(q_1) = \frac{\epsilon_0 I(q_1) - 1}{\epsilon_0 I(q_1) + 1} \, . \tag{23}$$

Finally, the total potential outside the metal is

$$\phi(\vec{q}_1, z) = \frac{2\pi Q}{\epsilon_0 q_1} [e^{-q_1|z+z_0|} + B(q_1)e^{q_1(z-z_0)}] \, ,$$

$$z < 0 \quad (24)$$

the second term being the induced potential $\phi'(\vec{q}_1, z)$, whereas the potential inside the metal is

$$\phi(\vec{q}_1, z) = \frac{2\pi Q}{q_1} e^{-q_1 z_0} \frac{2I(q_1, z)}{\epsilon_0 I(q_1) + 1}, \quad z > 0 \quad (25)$$

where[24]

$$I(q_1, z) = \frac{q_1}{\pi} \int_{-\infty}^{\infty} \frac{e^{iq_z z} dq_z}{q^2 \epsilon_l(\vec{q}, \omega)} \, . \tag{26}$$

It can be readily verified that for a local dielectric constant $[\epsilon_l(\vec{q}, \omega) \rightarrow \epsilon(\omega)]$, the above equations reduce to the usual image solutions. We find $I(q_1, z) = \epsilon^{-1} \exp(-q_1 z)$ and $I(q_1) = \epsilon^{-1}$, so the local induced potential in Eq. (24) is

$$\phi'(\vec{q}_1, z) = \frac{2\pi}{q_1} \left[\frac{\epsilon_0 - \epsilon}{\epsilon_0 + \epsilon} \right] \frac{Q}{\epsilon_0} e^{q_1(z-z_0)}, \quad z < 0$$

$$(27)$$

which, by comparing with Eq. (3b), is the potential due to a point image charge $Q(\epsilon_0 - \epsilon)/(\epsilon_0 + \epsilon)$ located at $+z_0$ in an infinite medium with dielectric constant ϵ_0. From Eq. (25), the local potential inside the metal

$$\phi(\vec{q}_1, z) = \frac{2\pi}{q_1} \left[\frac{2\epsilon}{\epsilon + \epsilon_0} \right] \frac{Q}{\epsilon} e^{-q_1(z+z_0)}, \quad z > 0$$

$$(28)$$

is the potential due to a point image charge $Q 2\epsilon/(\epsilon + \epsilon_0)$ located at $-z_0$ in an infinite medium with dielectric constant ϵ.

The potential in real space is found from Eq. (24) or (25) by an inverse Fourier transform of the form

$$\phi(\vec{\rho}, z) = \frac{1}{(2\pi)^2} \int \phi(\vec{q}_1, z) e^{i\vec{q}_1 \cdot \vec{\rho}} d^2 q_1 \, . \tag{29}$$

Using the axial symmetry of the potential (ϕ depends only on the magnitude q_1), the angular integration in $d^2 q_1 = q_1 dq_1 d\theta$ can be carried out, leaving the radial integration

$$\phi(\vec{\rho}, z) = \frac{1}{2\pi} \int_0^\infty \phi(q_1, z) J_0(q_1 \rho) q_1 dq_1 \, , \tag{30}$$

where $J_0(q_1 \rho)$ is the Bessel function of order zero.

We now analyze the behavior of the normal component of the electric field at the surface. From Eq. (15) we find

$$\mathscr{E}_z(\vec{q}) = - \frac{2iq_z D_z(\vec{q}_1, 0^+)}{q^2 \epsilon_l(\vec{q}, \omega)} \, . \tag{31}$$

Applying the theorem (12) to Eq. (31), we immediately find the electric field just inside the surface:

$$E_z(\vec{q}_1, z = 0^+) = D_z(\vec{q}_1, 0^+)/\epsilon_1 \, , \tag{32}$$

where

$$\epsilon_1 = \lim_{q \to \infty} \epsilon_l(\vec{q}, \omega) \tag{33}$$

is the local background dielectric constant of the metal. From the continuity of D_z it follows that

$$\epsilon_0 E_z(\vec{q}_1, 0^-) = \epsilon_1 E_z(\vec{q}_1, 0^+) \, , \tag{34}$$

and that the nonlocal part of the polarization (or the current density) $P_z = (D_z - \epsilon_1 E_z)/4\pi$ inside the metal must vanish at the surface. The calculations in Sec. III will be applied to a metal with no local background dielectric constant ($\epsilon_1 = 1$), and a vacuum as the second medium ($\epsilon_0 = 1$). In this particular situation both D_z and E_z are continuous and the normal component of the current density vanishes at $z = 0$. The surface polarization charge that would exist in a local theory is replaced by a volume charge density inside the metal.

B. Induced electric field of a dipole

We now place a dipole outside the metal, instead of a single point charge. This dipole induces charges inside the metal which are sources of the potential ϕ' and an induced field $\vec{E}'$ outside the metal. The field $\vec{E}'$ will be determined at the site of the dipole.

Starting with the induced potential $\phi'(\vec{q}_1, z)$ for a single charge, the second term in Eq. (24), we find the potential for a dipole in the z direction by adding potentials for a charge Q at $(0, 0, -z_0)$ and a charge $-Q$ at $(0, 0, -z_0 - \Delta)$. Expanding to first order in Δ and introducing the dipole moment $p_z = Q\Delta$, we find

$$\phi'(\vec{q}_1, z) = \frac{2\pi p_z}{\epsilon_0} B(q_1) e^{q_1(z-z_0)} \, . \tag{35}$$

We take the inverse Fourier transform as in Eq. (29) to find the potential at the arbitrary point $(\vec{\rho}, z)$. Differentiating with respect to z gives the electric field

$$E_z'(\vec{\rho}, z) = -\frac{p_z}{2\pi\epsilon_0} \int q_1 B(q_1) e^{q_1(z-z_0)} e^{i\vec{q}_1 \cdot \vec{\rho}} d^2 q_1 ,$$

(36)

and evaluating this at $\vec{\rho} = 0$, $z = -z_0$ gives

$$E_z' \equiv E_z'(0, -z_0) = -\frac{p_z}{\epsilon_0} \int_0^\infty B(q_1) e^{-2q_1 z_0} q_1^2 dq_1 .$$

(37)

The potential ϕ' for a dipole in the x direction is found similarly by adding potentials for point charges Q at $(0,0,-z_0)$ and $-Q$ at $(-\Delta,0,-z_0)$. Differentiating with respect to x, we find the induced field

$$E_x'(\vec{\rho}, z) = -\frac{p_x}{2\pi\epsilon_0} \int \frac{q_x^2}{q_1} B(q_1) e^{q_1(z-z_0)} e^{i\vec{q}_1 \cdot \vec{\rho}} d^2 q_1 ,$$

(38)

and, at the site of the dipole,

$$E_x' \equiv E_x'(0, -z_0) = -\frac{p_x}{2\epsilon_0} \int_0^\infty B(q_1) e^{-2q_1 z_0} q_1^2 dq_1 ,$$

(39)

a result differing from Eq. (37) only by the factor $\frac{1}{2}$. Equations (37) and (39) can be combined to give the total induced field at the site of the dipole:

$$\vec{E}' = -F(z_0, \omega)(\tfrac{1}{2} p_x \hat{i} + p_z \hat{k}) ,$$

(40)

where

$$F(z_0, \omega) = \epsilon_0^{-1} \int_0^\infty B(q_1) e^{-2q_1 z_0} q_1^2 dq_1 .$$

(41)

C. Renormalized polarizability of a dipole oscillator

The dipole will be assumed to have an isotropic frequency-dependent polarizability $\alpha_0(\omega)$. Let $\vec{E}_0$ be the electric field (oscillating at frequency ω) that would exist at the point $(0,0,-z_0)$ outside the metal when the dipole is absent. When the polarizable dipole is placed at this point, the field acting on the dipole is the sum of the applied field E_0 and the induced field $\vec{E}'$; that is,

$$\vec{p} = \alpha_0(\omega)(\vec{E}_0 + \vec{E}')$$

(42)

$$= \alpha_0(\omega)[\vec{E}_0 - F(z_0, \omega)(\tfrac{1}{2} p_x \hat{i} + p_z \hat{k})] ,$$

(43)

where we have assumed that $\vec{E}_0$, and hence $\vec{E}'$, lie in the $x - z$ plane. The solution of Eq. (43) for p_x and p_z can be written

$$p_j = \alpha_j(\omega) E_{0j}, \quad j = x, z$$

(44)

where

$$\alpha_j(\omega) = \frac{\alpha_0(\omega)}{1 + n_j \alpha_0(\omega) F(z_0, \omega)} ,$$

(45)

with $n_x = \frac{1}{2}$, $n_z = 1$. The quantities $\alpha_x(\omega)$ and $\alpha_z(\omega)$ are components of the renormalized polarizability, i.e., the polarizability α_0 modified by the interaction of the dipole with its "image" in the metal. It will be seen in Sec. III that nonlocality in the response of the metal has a significant effect on the form of $F(z_0, \omega)$ and hence, on the renormalized polarizability.

III. CALCULATIONS USING HYDRODYNAMIC DIELECTRIC CONSTANT

A. Induced field at the site of the dipole

We describe the metal using the hydrodynamic dielectric constant

$$\epsilon_l(\vec{q}, \omega) = 1 - \frac{\omega_p^2}{\tilde{\omega}^2 - \beta^2 q^2} ,$$

(46)

where $\tilde{\omega}^2 = \omega(\omega + i/\tau)$, τ being a phenomenological relaxation time, ω_p is the plasma frequency, $\beta^2 = \frac{3}{5} v_F^2$, and $q^2 = q_1^2 + q_z^2$. Although this dielectric constant becomes invalid at low frequencies and does not contain electron-hole pair excitations, it gives a qualitatively correct description of the bulk-plasmon and surface-plasmon dispersion. An advantage of using Eq. (46) rather than a more realistic dielectric constant (such as Lindhard-Mermin) is that it allows many expressions in the previous sections to be evaluated analytically and makes the physical interpretation of the results more transparent.

Equation (22) can be easily evaluated using Eq. (46). We find

$$I(q_1) = 1 + \frac{\omega_p^2}{\tilde{\omega}^2 - \omega_p^2}\left[1 - \frac{q_1}{\Gamma}\right] ,$$

(47)

where

$$\Gamma^2 = q_1^2 + \frac{\omega_p^2 - \tilde{\omega}^2}{\beta^2} .$$

(48)
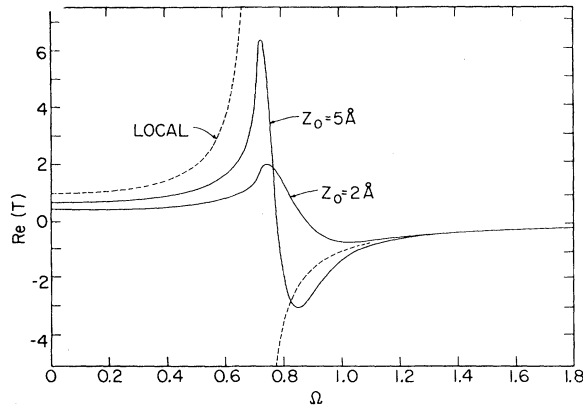
FIG. 1. ReT as a function of $\Omega = \omega/\omega_p$ for a local metal (dashed curve) and a nonlocal metal with $z_0 = 2$ and 5 Å (solid curves). A nearly vertical portion of the dashed curve at $\Omega \approx 1/\sqrt{2}$ is not shown.

Equation (23), with $\epsilon_0 = 1$, then gives

$$B(q_1) = \frac{q_1 - \Gamma}{q_1 + A\Gamma} , \qquad (49)$$

where $A = (\epsilon_{loc} + 1)/(\epsilon_{loc} - 1)$ and $\epsilon_{loc} = 1 - \omega_p^2/\tilde{\omega}^2$. Equation (49) is then used in Eq. (37) to find E_z', the induced field at the site of a dipole in the z direction:

$$E_z' = \frac{p_z}{4|z_0|^3} T , \qquad (50)$$

where

$$T = \frac{1}{A} \left[1 - \frac{4\beta}{\omega_p}(A + 1) \int_0^\infty e^{-2u} \frac{u^3}{Ab + \beta u/\omega_p} du \right] \qquad (51)$$

with

$$b = [(\beta/\omega_p)^2 u^2 + (1 - \tilde{\Omega}^2)|z_0|^2]^{1/2} ,$$

$$\tilde{\Omega}^2 = \tilde{\omega}^2/\omega_p^2 .$$

In the local limit, $\beta = 0$ and Eq. (51) reduces to

$$T = \frac{1}{A} = \frac{\epsilon_{loc} - 1}{\epsilon_{loc} + 1} . \qquad (52)$$

· We have calculated the real and imaginary parts of T as functions of the dimensionless frequency ratio $\Omega = \omega/\omega_p$ for several values of the distance z_0, using the electron density parameter $r_s = 2$, corresponding to Al. In order to remove the singularity in T in the local limit when $\Omega = 1/\sqrt{2}$, the relaxation time τ is given a finite value: $\gamma \equiv (\omega_p\tau)^{-1}$

$= 10^{-3}$.

The results are shown in Figs. 1 and 2. The most prominent feature, most easily seen in Fig. 2, is that the sharp resonance in the local limit at the frequency $\Omega = 1\sqrt{2}$ is broadened by nonlocality. The width of the resonance increases as the distance z_0 of the dipole from the surface decreases, and the resonance is broadened asymmetrically to the high-frequency side.

Two physical effects contribute to this broadening: (1) dispersion of the surface plasmon and (2) additional energy dissipation when $\Omega > 1$ due to coupling to bulk plasmons. In order to explain effect (1) qualitatively, we must first note that at a given frequency the induced potential can be considered as the superposition of surface-plasmon potentials with different values of the wave vector $\vec{q}_1$. According to Eq. (3b) the range of q_1 values for the potential of the external charge is $\Delta q_1 \sim z_0^{-1}$, so as the charge approaches the surface the range of q_1 increases. The q_1 Fourier component of the induced potential has a resonant peak at a frequency equal to that of a surface plasmon at this value of q_1. If a local free-electron dielectric constant is used, the surface-plasmon frequency is $\omega_s = \omega_p/\sqrt{2}$ and is independent of q_1. Therefore each Fourier component of the induced potential has a resonance at the same frequency $\omega_p/\sqrt{2}$, and so does the entire induced potential. With a nonlocal dielectric constant, the surface plasmon has dispersion: The frequency $\omega_s = \omega_p/\sqrt{2}$ at $q_1 = 0$ and increases at large values of q_1. Hence the small-q_1 Fourier components of the induced potential respond resonantly at $\omega \sim \omega_p/\sqrt{2}$, and the large-$q_1$ Fourier components at frequencies $\omega > \omega_p/\sqrt{2}$. This explains why ϕ', and hence the field E_z', has a broad asymmetric resonance beginning at $\omega_p/\sqrt{2}$ and extending to higher frequencies, the width increasing as z_0 decreases.

The preceding statements can be verified by noting that the Fourier component $\phi'(\vec{q}_1, z)$ of the induced potential, given by the second term of Eq. (24), contains the factor $B(q_1)$ defined 'n Eq. (23). The condition that the denominator $G(q_1,\omega)$ of $B(q_1)$ vanish, i.e., $G(q_1,\omega) \equiv \epsilon_0 I(q_1) + 1 = 0$ gives the surface-plasmon dispersion relation $\omega = \omega_s$ a complex frequency, as a function of real q_1. When ω is real, $G(q_1,\omega)$ does not vanish but becomes small and purely imaginary when Re$G(q_1,\omega) = 0$ or $\omega \sim$ Reω_s, producing a peak in Im$B(q_1)$.

Effect (2), the coupling to bulk plasmons, appears as an additional contribution to ImT when $\omega > \omega_p$ or $\Omega > 1$. It is most easily seen in Fig. 2
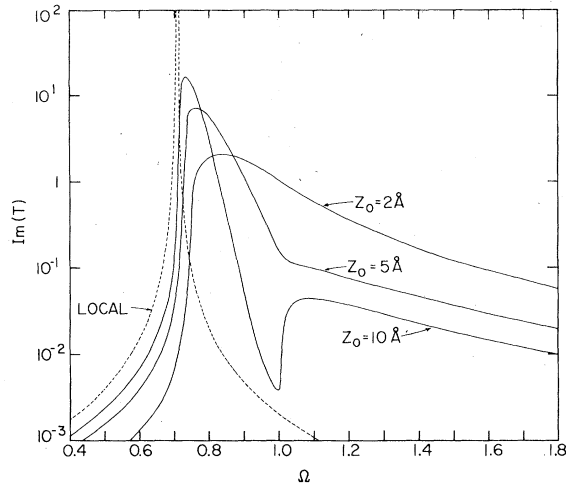
FIG. 2. $\mathrm{Im}T$ as a function of $\Omega = \omega/\omega_p$ for a local metal (dashed curve) and a nonlocal metal with $z_0 = 2$, 5, and 10 Å (solid curves).

for large distances z_0 ($z_0 = 10$ Å and $z_0 = 5$ Å). Although this effect also exists for $z_0 = 2$ Å, the additional contribution to $\mathrm{Im}T$ is hidden by the very broad resonance arising from effect (1). The coupling to bulk plasmons is associated with an increase of $\mathrm{Im}I(q_1)$ when $\omega > \omega_p$; this contributes to $\mathrm{Im}G(q_1,\omega) = \mathrm{Im}\epsilon_0 I(q_1)$ and finally, to $\mathrm{Im}T$. As is evident from Eq. (22), $\mathrm{Im}I(q_1)$ involves an integration over the longitudinal energy-loss function $\mathrm{Im}[-1/\epsilon_l(q,\omega)]$, which has a bulk-plasmon energy-loss peak when $\omega > \omega_p$. A similar coupling to bulk plasmons is responsible for additional optical absorption of p-polarized light when $\omega > \omega_p$.

Equation (50) for the induced field can be written

$$E_z' = \frac{p_z}{4A \, |z_0 + z'|^3} \, . \tag{53}$$

This is of the same form as the local induced field, except that the distance z_0 is replaced by $z_0 + z'$, where z' is a complex distance which includes all effects of nonlocality; i.e., for a local metal $z' = 0$. Equation (53) can be interpreted as follows: The field at the site of a dipole located at $-z_0$ outside the metal is given by using the same image dipole as for a local metal, but locating the image dipole at the complex position $z_0 + 2z'$. Comparison of Eqs. (50) and (53) immediately gives an expression for z':

$$z' = z_0[(AT)^{-3} - 1] \, . \tag{54}$$

In the limit as $z_0 \to \infty$, T can be found by taking $b \approx |z_0| (1 - \widetilde{\Omega}^2)^{1/2}$ and neglecting the term $\beta u /\omega_p$ in the denominator of Eq. (51). The integra-
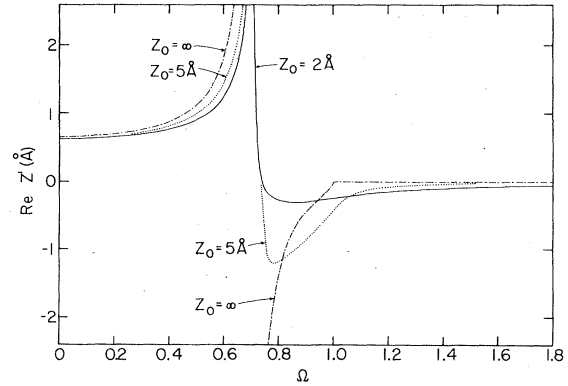

FIG. 3. $\mathrm{Re}z'$, in Å, as a function of $\Omega = \omega/\omega_p$ for $z_0 = \infty$ (dot-dashed curve), $z_0 = 5$ Å (dotted curve), and $z_0 = 2$ Å (solid curve). A nearly vertical portion of the dot-dashed curve at $\Omega \approx 1/\sqrt{2}$ is not shown.

tion in Eq. (51) can then be done analytically, and Eq. (54) gives

$$z' \big|_{z_0 \to \infty} = \frac{\beta}{\omega_p} \frac{(1 - \widetilde{\Omega}^2)^{1/2}}{1 - 2\widetilde{\Omega}^2} \, . \tag{55}$$

From Eq. (55) it follows that $\mathrm{Im}z' \big|_{z_0 \to \infty}$ has a sharp peak at $\Omega = 1/\sqrt{2}$ originating from the denominator, $1 - 2\widetilde{\Omega}^2$, and a broad shoulder for $\Omega > 1$ originating from $(1 - \widetilde{\Omega}^2)^{1/2}$, these effects arising from the surface plasmon and coupling to bulk plasmons, respectively.

Figures 3 and 4 show $\mathrm{Re}z'$ and $\mathrm{Im}z'$ for $z_0 \to \infty$ (dot-dashed lines) and also for several smaller values of z_0. As z_0 decreases, the surface-plasmon peak in $\mathrm{Im}z'$ at $\Omega = 1/\sqrt{2}$ broadens asymmetrically to high frequencies, and the shoulder at $\Omega \gtrsim 1$ becomes obscured by the broad surface-plasmon peak.
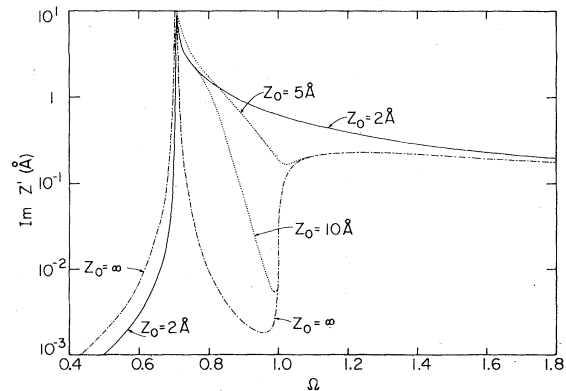

FIG. 4. $\mathrm{Im}z'$, in Å, as a function of $\Omega = \omega/\omega_p$ for $z_0 = \infty$ (dot-dashed curve), $z_0 = 10$ and 5 Å (dotted curves) and $z_0 = 2$ Å (solid curve).

Using a self-consistent model of an Al surface with a smooth density profile, Feibelman[12] also has calculated $\text{Re}z'|_{z_0\to\infty}$ and $\text{Im}z'|_{z_0\to\infty}$. Feibelman's result for $\text{Re}z'|_{z_0\to\infty}$ has some similarity to ours: There is a singularity at $\Omega = 1/\sqrt{2}$, but his value becomes positive for Ω in the range $0.74 < \Omega < 1$, whereas ours remains negative in the entire range $(1/\sqrt{2}) < \Omega < 1$. His values of $\text{Re}z'|_{z_0\to\infty}$ are smaller than ours by a factor of about 5. Feibelman's result for $\text{Im}z'|_{z_0\to\infty}$ is in complete disagreement with ours: He finds a singular behavior at $\Omega = 1/\sqrt{2}$ that has a sign change, whereas we find a positive peak at $\Omega = 1/\sqrt{2}$. Furthermore, he finds no contribution to $\text{Im}z'$ from bulk plasmons when $\Omega > 1$. We are unable to understand why Feibelman's calculation for a relatively accurate model of a metal surface should yield results so different from those we have found using the much simpler SCIB hydrodynamic model. This disagreement is especially puzzling since our results have features that have such obvious physical interpretations.

B. Renormalized polarizability of a dipole

We assume that the unrenormalized polarizability of the dipole has a natural resonance frequency ω_0, unit oscillator strength, and zero width:

$$\alpha_0(\omega) = \frac{e^2/m}{\omega_0^2 - \omega^2} . \tag{56}$$

We place this dipole in vacuum at a distance z_0 from the metal surface and calculate the renormalized polarizability $\alpha_z(\omega)$ from Eq. (45). A comparison of Eqs. (37), (41), and (50) shows that $F(z_0,\omega) = -T/4z_0^3$. If we introduce the dimensionless natural resonance frequency $\Omega_0 = \omega_0/\omega_p$ and renormalized polarizability $\tilde{\alpha} = (m\omega_p^2/e^2)\alpha_z(\omega)$, we can rewrite Eq. (45) as

$$\tilde{\alpha} = [\Omega_0^2 - \Omega^2 - (g/z_0)^3 T]^{-1} , \tag{57}$$

where $g = (r_s a_0)^3/12 = 0.98$ Å^3 for Al ($r_s = 2$ and $a_0 = 0.529$ Å). We have calculated $\tilde{\alpha}$ only for one distance, $z_0 = 2$ Å.

Suppose that we use a local dielectric constant for the metal and neglect damping. Then $T = (\epsilon_{\text{loc}} - 1)/(\epsilon_{\text{loc}} + 1) = (1 - 2\Omega^2)^{-1}$. We can easily find the frequencies Ω (which we denote Ω') for which the quantity in square brackets in Eq. (57) becomes zero; i.e., the poles of $\tilde{\alpha}$ occur at Ω'. In Fig. 5 Ω' is shown as a function of Ω_0. It is apparent that the two solutions for Ω' can be considered as a "natural" or unrenormalized branch

$\Omega' = \Omega_0$ and a surface-plasmon branch $\Omega' = 1/\sqrt{2}$ which interact repulsively in the crossing region $\Omega_0 \sim \Omega' \sim 1/\sqrt{2}$ so that there is, in fact, no crossing. The oscillator strength, which is not shown in Fig. 4, is concentrated in the "natural" branch; i.e., in the low-frequency mode when $\Omega_0 \lesssim 1/\sqrt{2}$ and in the high-frequency mode when $\Omega_0 \gtrsim 1/\sqrt{2}$, with a continuous transfer of oscillator strength from one mode to the other in the interaction region $\Omega_0 \sim 1/\sqrt{2}$.

In Figs. 6(a) — 6(d), we have plotted $\text{Im}\tilde{\alpha}$ as a function of Ω for the selected values $\Omega_0 = 0.6, 0.7, 0.8$, and 1.0, and with the damping factor $\gamma = 10^{-3}$ for the metal. The dashed curves, which show the local results, have peaks at frequencies that are the same as the Ω' frequencies shown in Fig. 5. The transfer of oscillator strength discussed in the preceding paragraph is also evident. The damping in the metal accounts for the finite width of the peaks, as the free dipole oscillator is assumed to have zero width.

Figures 6(a) — 6(d) also show nonlocal results for $\text{Im}\tilde{\alpha}$, obtained by using nonlocal values of T calculated from Eq. (51) in Eq. (57). The behavior of $\text{Im}\tilde{\alpha}$ can be understood qualitatively for examining the frequency dependence of $\text{Re}T$ and $\text{Im}T$ for $z_0 = 2$ Å as shown in Figs. 1 and 2. The asymmetric broadening of the peak in $\text{Im}T$ produces strong damping of the resonances in $\tilde{\alpha}$ that lie at frequencies higher than $\Omega = 1/\sqrt{2}$. Moreover, the magnitude of $\text{Re}T$, which shifts the frequency of resonance, is generally smaller in the nonlocal calculation. Thus in Fig. 6(a), for example, the low-frequency nonlocal peak in $\text{Im}\tilde{\alpha}$ at $\Omega = 0.59$ lies much closer to the natural resonance frequency
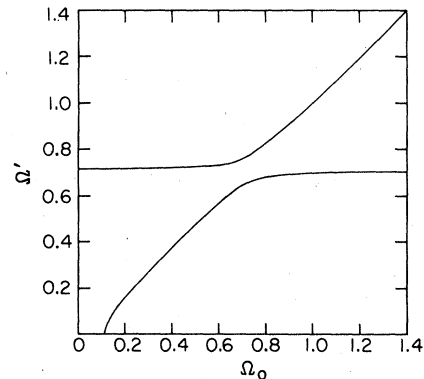
FIG. 5. Resonance frequencies $\Omega' = \omega'/\omega_p$ of the renormalized dipole polarizability as a function of the natural dipole resonance frequency $\Omega_0 = \omega_0/\omega_p$, for a local metal.
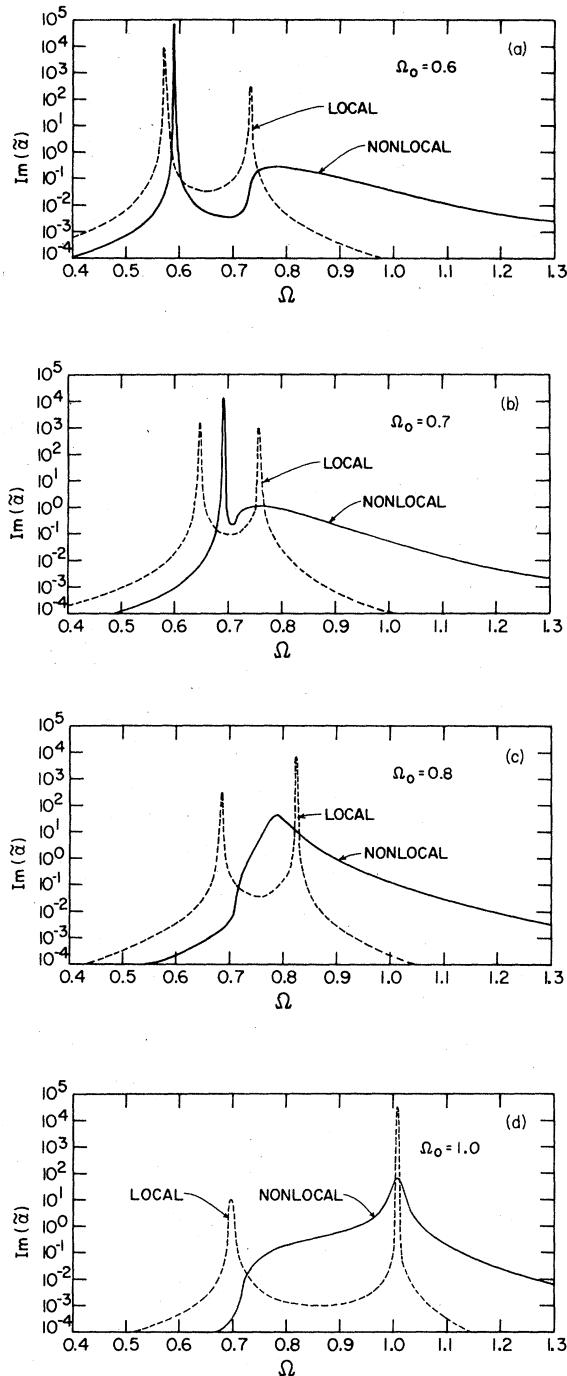
FIG. 6. (a)—(d) Renormalized polarizability, $\mathrm{Im}\tilde{\alpha}$, as a function of $\Omega = \omega/\omega_p$, for $z_0 = 2$ Å and for various values of the natural dipole resonance frequency $\Omega_0 = \omega_0/\omega_p$. The dashed and solid curves are for a local and nonlocal metal, respectively. (a): $\Omega_0 = 0.6$; (b): $\Omega_0 = 0.7$; (c): $\Omega_0 = 0.8$; (d): $\Omega_0 = 1.0$.

$\Omega_0 = 0.60$ than does the corresponding local peak. A general feature of the nonlocal results is that only

one peak in $\mathrm{Im}\tilde{\alpha}$ is large enough to be detectable experimentally. This is especially significant for $\Omega_0 = 0.7$ [Fig. 6(b)], where the local theory gives two well-separated peaks with almost equal oscillator strengths but the nonlocal theory gives essentially only a single peak at $\Omega = 0.69$.

IV. CONCLUSION

We have shown that when a dipole is within a few Å of a metal surface, nonlocality of the metal is important in calculating the image field and renormalized polarizability. It will be of interest to see how the conclusions of the present calculation, based on a hydrodynamic dielectric function for the metal, are altered if the more realistic Lindhard-Mermin dielectric function is used.

The role of nonlocality has been emphasized by Weber and Ford[20] in connection with surface-enhanced Raman scattering, but they have not considered the frequency dependence of the unrenormalized polarizability α_0. We have seen that the frequency dependence of the renormalized polarizability changes significantly as the resonance frequency of α_0 varies, so this should be included in the theory of surface-enhanced Raman scattering.

The connection between the present treatment and that of Feibelman,[12] who has used a more accurate model of the metal surface, is unclear. Since the surface-plasmon dispersion depends on the electron density profile at the surface, one would not expect our SCIB model, in which the electron density drops discontinuously to zero, to give the correct shape of the broadened induced-field singularity, as shown in Fig. 2, for example. However, one would expect the SCIB model to become seriously invalid only for z_0 as small as $1-2$ Å, a distance comparable to the actual width of the electron density profile.[25] Thus, our disagreement with the results of Feibelman even for large distances is puzzling.

This work bears directly on the theory of differential surface reflectance spectroscopy of atoms adsorbed on metal surface. An existing theory of this effect is being extended so as to include nonlocality of the metal, and the results will be reported in the future.

APPENDIX

We shall derive expressions for the potential when a charge Q is added *inside* the metal at the point $x = y = 0$, $z = z_0 > 0$. As before, the medium outside the metal $(z < 0)$ has a local dielectric constant ϵ_0.

Since the total potential outside the metal satisfies Laplace's equation, it is of the same form as the induced potential in Eq. (6):

$$\phi(\vec{q}_1, z) = C_1 e^{q_1 z}, \quad z < 0 . \tag{A1}$$

From Eq. (A1) we find the displacement

$$D_z(\vec{q}_1, z) = -\epsilon_0 q_1 C_1 e^{q_1 z}, \quad z < 0 . \tag{A2}$$

To determine the potential inside the metal we again use the SCIB approximation: Extend the metal throughout all space with the requirement that the z components of $\vec{D}$ and $\vec{E}$ be odd functions of z, or that the potential and charge distributions be even functions of z. With the true charge Q at $x = y = 0$, $z = z_0$, we must include a fictitious symmetric image charge Q at $x = y = 0$, $z = -z_0$. There is also a fictitious charge layer at $z = 0$, as before.

The two point charges are sources of the "potential"

$$\phi_D(\vec{q}) = \frac{4\pi Q}{q^2} (e^{-iq_z z_0} + e^{iq_z z_0}) . \tag{A3}$$

Dividing Eq. (A3) by $\epsilon_l(\vec{q}, \omega)$ and taking the inverse Fourier transform as in Eq. (16), we find

$$\phi(\vec{q}_1, z) = 4Q \int_{-\infty}^{\infty} \frac{\cos q_z z_0}{q^2 \epsilon_l(q_1 \omega)} e^{iq_z z} dq_z . \tag{A4}$$

Because of symmetry, the "potential" ϕ_D of Eq. (A3) does not contribute to the normal component of D_z at the surface.

The fictitious surface charge layer is treated just as in Eqs. (7)−(17); it is the source of $D_z(q_1, 0^+)$ and produces the potential $\phi(\vec{q}_1, 0^+)$ as in Eq. (17). Just inside the surface of the metal the potential is, therefore, the sum of Eqs. (17) and (A4).

From the continuity of ϕ and D_z at $z = 0$ in the actual system, we find

$$C_1 = 4Q \int_{-\infty}^{\infty} \frac{\cos q_z z_0}{q^2 \epsilon_l(q, \omega)} dq_z$$

$$+ \frac{1}{\pi} D_z(\vec{q}_1, 0^+) \int_{-\infty}^{\infty} \frac{dq_z}{q^2 \epsilon_l(q, \omega)} \tag{A5}$$

and

$$-\epsilon_0 q_1 C_1 = D_z(\vec{q}_1, 0^+) . \tag{A6}$$

Equations (A5) and (A6) are readily solved for the unknown quantities C_1 and $D_z(q_1, 0^+)$, and the final expressions for the potentials are

$$\phi(\vec{q}_1, z) = \begin{cases} \dfrac{2\pi Q}{q_1} \left[K(q_1, z) - \dfrac{\epsilon_0 K(q_1)}{\epsilon_0 I(q_1) + 1} I(q_1, z) \right], \\ \qquad\qquad\qquad\qquad\qquad z > 0 \quad \text{(A7)} \\ \dfrac{2\pi Q}{q_1} \dfrac{K(q_1)}{\epsilon_0 I(q_1) + 1} e^{q_1 z}, \quad z < 0 \quad \text{(A8)} \end{cases}$$

where $I(q_1)$ and $I(q_1, z)$ are defined in Eqs. (22) and (26), and

$$K(q_1, z) = \frac{q_1}{\pi} \int_{-\infty}^{\infty} \frac{2\cos q_z z_0}{q^2 \epsilon_l(\vec{q}, \omega)} e^{iq_z z} dq_z , \tag{A9}$$

$$K(q_1) = \frac{q_1}{\pi} \int_{-\infty}^{\infty} \frac{2\cos q_z z_0}{q^2 \epsilon_l(\vec{q}, \omega)} dq_z . \tag{A10}$$

In Eq. (A7) the first term is the potential produced by the real charge and its symmetric image, whereas the second term is the potential produced by the fictitious surface charge layer at $z = 0$. By taking inverse Fourier transforms as in Eqs. (29) or (30) we find the potentials in real space, $\phi(\vec{p}, z)$.

When $\epsilon_l(\vec{q}, \omega) \rightarrow \epsilon(\omega)$, Eqs. (A7) and (A8) reduce to the correct local limit. In this limit we find

$$K(q_1, z) = \epsilon^{-1} [\exp(-q_1 |z + z_0|) \\ + \exp(-q_1 |z - z_0|)]$$

and $K(q_1) = 2\epsilon^{-1} \exp(-q_1 z_0)$, so Eq. (A7) reduces to

$$\phi(\vec{q}_1, z) = \frac{2\pi Q}{q_1 \epsilon} \left[e^{-q_1 |z - z_0|} + \frac{\epsilon - \epsilon_0}{\epsilon + \epsilon_0} e^{-q_1 |z + z_0|} \right],$$

$$z > 0 \quad \text{(A11)}$$

the sum of the potentials due to the real charge Q at z_0 and an image charge $Q(\epsilon - \epsilon_0)/(\epsilon + \epsilon_0)$ at

$-z_0$, in a medium ϵ, while Eq. (A8) reduces to

$$\phi(\vec{q}_1,z) = \frac{2\pi Q}{q_1\epsilon_0} \frac{2\epsilon_0}{\epsilon + \epsilon_0} e^{-q_1|z-z_0|}, \quad z < 0 . \quad \text{(A12)}$$

the potential due to an image charge $Q 2\epsilon_0/(\epsilon + \epsilon_0)$ at z_0 in a medium ϵ_0.

[1]D. L. Jeanmaire and R. P. Van Duyne, J. Electroanal. Chem. **84**, 1 (1977).

[2]F. W. King, R. P. Van Duyne, and G. C. Schatz, J. Chem. Phys. **69**, 4472 (1978).

[3]S. Efrima and H. Metiu, J. Chem. Phys. **70**, 1602 (1979); **70**, 2297 (1979).

[4]J. E. Cunningham, D. Greenlaw, J. L. Erskine, R. P. Layton, and C. P. Flynn, J. Phys. F **7**, L281 (1977).

[5]J. E. Cunningham, D. Greenlaw, C. P. Flynn, and J. L. Erskine, Phys. Rev. Lett. **42**, 328 (1979).

[6]H. Morawitz, Phys. Rev. **187**, 1792 (1969).

[7]H. Morawitz and M. R. Philpott, Phys. Rev. B **10**, 4863 (1974).

[8]A. Bagchi, R. G. Barrera, and B. B. Dasgupta, Phys. Rev. Lett. **44**, 1475 (1980).

[9]D. E. Beck and V. Celli, Phys. Rev. B **2**, 2955 (1970).

[10]D. E. Beck, V. Celli, G. Lo Veccio, and A. Magnaterra, Nuovo Cimento **68B**, 230 (1970).

[11]W. C. Meixner and P. R. Antoniewicz, Phys. Rev. B **13**, 3276 (1976).

[12]P. J. Feibelman, Phys. Rev. B **23**, 2629 (1981).

[13]G. Korzeniewski, T. Maniv, and H. Metiu, Chem. Phys. Lett. **73**, 212 (1980); G. Korzeniewski, T. Maniv, and H. Metiu (unpublished); T. Maniv and H. Metiu, J. Chem. Phys. **72**, 1996 (1980).

[14]R. Fuchs and K. L. Kliewer, Phys. Rev. **185**, 905 (1969).

[15]G. Mukhopadhay and S. Lundqvist, Phys. Scr. **17**, 69 (1978).

[16]A. Sommerfeld, Ann. Phys. (Leipzig) **81**, 1135 (1926); **28**, 665 (1909); *Partial Differential Equations of Phy-*

sics (Academic, New York, 1949).

[17]The methods of Sommerfeld cannot, however, be generalized readily to a charge embedded in the nonlocal medium, as we have done in the Appendix.

[18]R. R. Chance, A. Prock, and R. Silbey, in *Advances in Chemical Physics*, edited by I. Prigogine and S. A. Rice (Wiley, New York, 1978), Vol. XXXVII, p. 1.

[19]K. H. Tews, Ann. Phys. (Leipzig) **29**, 97 (1973).

[20]W. H. Weber and G. W. Ford, Phys. Rev. Lett. **44**, 1774 (1980).

[21]G. S. Agarwal and H. O. Wolmer, Phys. Status Solidi **85**, 301 (1978).

[22]It should be emphasized that this fictitious charge layer is present only in the infinitely extended metal and is related to the discontinuity of D_z at $z = 0$. In the physical system, D_z is continuous at $z = 0$.

[23]D. L. Johnson and P. R. Rimbey, Phys. Rev. B **14**, 2398 (1976).

[24]Quantities such as $I(q_1)$ and $I(q_1,z)$ dpend on ω, although this is not indicated explicitly.

[25]In Ref. 13, Korzeniewski *et al.* make a detailed comparison of their infinite-barrier model with an SCIB model of a metal having $r_s = 5$ at a single frequency $\Omega = 0.61$ and conclude that the SCIB model gives qualitatively correct results if the dipole is more than about 2 Å from the surface. They also find that it is most accurate to locate the $z = 0$ plane in the SCIB model so it coincides with the edge of a uniform positive jellium background located to give charge neutrality in the infinite-barrier model; this is about 1.6 Å from the infinite-barrier position.